

# Intelligent Detection Technology of Over-Under Excavation in Mining Tunnel Based on 3D Laser Scanning

Chenglong Qi\*, Yan Li, Yi Zhuo, Yao Li, Rongzheng Zheng  
China Railway Design Corporation, Tianjin 300308, China

\*Corresponding author: qichenglong@live.cn

## ABSTRACT

To improve the level of over-under excavation detection in construction process of mining tunnels, scholars domestic and abroad have combined 3D laser scanning with other information technology to achieve certain research results. However, the existing research results mainly use sectional method, without fully taking advantage of 3D technology. To address these issues, this paper uses algorithms such as registration, cutting, denoising, and downsampling for pre-processing of laser scanning point clouds. Then, point clouds are transformed into spatial meshes through cluster and BPA algorithms. With the help of triangular mesh projection and prism volume integration, 3D over-under excavation condition is calculated. Through application verification in actual engineering projects, it is achieved that the over-under excavation detection process during construction phase for mining tunnels are automated and intelligent.

**Keywords:** Tunnel; Point cloud; Denoise; Over-under excavation; Ball Pivoting Algorithm; Triangulation

## 1. INTRODUCTION

Due to errors that may occur during the survey and construction processes of mining tunnels, over-under excavation detection is required to determine if the clearance meets design requirements<sup>[1][2]</sup>. Traditional methods for over-under excavation detection in tunnels mainly rely on total stations, cross-sectional instruments, etc., to measure excavation sections point by point and surface by surface. However, these methods have shortcomings such as discrete points, large intervals, and missing in under-excavation detection.

To address above challenges, scholars domestic and abroad have conducted a series of studies on over-under excavation detection techniques by combining laser scanning with other information-based methods. Y. Li<sup>[3]</sup> used 3D laser scanning to collect sectional excavation data, and calculated over-under excavation volume, over-under excavation area, average linear over-under excavation amount, over-under excavation volume, and over-under excavation volume per meter according to algorithm researched in his paper. L. Xu<sup>[4]</sup> projected the sectional point cloud and used convex hull extraction method to automatically extract point cloud contour line, fit design section with measured section, determine the shortest distance between aforementioned two sections, and automatically calculate over-under excavation volume and direction value. X.L. Zheng<sup>[5]</sup> collected tunnel 3D point cloud data and conducted coordinate conversion to calculate axis of the tunnel and extract cross-sections, detect over-excavation and under-excavation zones, using the concept of infinite element to calculate over-under excavation amount in each zone.

In summary, current intelligent construction quality inspection of tunnel engineering is mainly carried out through point cloud processing methods, taking excavation cross-sections as research objects, and using point and line distance calculations to achieve over-under excavation index. Essentially, current methods are still two-dimensional technologies. Therefore, this paper uses algorithms such as cutting, noise reduction, completion, and downsampling to complete point cloud preprocessing, converts point clouds into spatial triangulations through clustering and BPA algorithms, exploiting triangulated mesh projection and prism volume integration to calculate over-under excavation volume. This paper will elaborate on key technologies of point cloud data preprocessing and three-dimensional over-under excavation calculation involved in this process, and verify above technologies through actual engineering projects.

## 2. POINT CLOUD PREPROCESSING

Due to the large amount of primitive point cloud data directly obtained by sensors, it often contains some noise information, and the spatial range often exceeds bounds of interest. Therefore, some preprocessing work is usually required in advance, including registration, segmentation, noise reduction, completion, downsampling<sup>[6]</sup> to improve the effectiveness and efficiency of over-under excavation calculation. This section selects some key technologies to analyze.

### 2.1 Point cloud registration based on ICP algorithm

Due to limited scanning range of 3D laser scanners, it is difficult to cover entire detection zone of the tunnel. Therefore, it is necessary to scan at multiple locations. In order to integrate point clouds obtained from multiple views into one integral point cloud, it is necessary to register point clouds obtained by laser scanner at different positions.

ICP algorithm is selected to implement point cloud registration<sup>[7]</sup>. The principle of this algorithm is: first, calculate the distance between each point and the target point cloud, matching each point with nearest one, which satisfies prerequisite for registration algorithm. After each point obtains a corresponding mapping point, the corresponding point set registration algorithm is to be carried out. This algorithm mainly uses solved rigid transformation matrix in global coordinate system to perform spatial transformation on point cloud data sets from different views with their own independent coordinate systems, in order to achieve the goal of converting point cloud data into the same coordinate system<sup>[8]</sup>.

### 2.2 Point cloud segmentation based on spatial vector analysis

Spatial scale of registered point cloud data often exceeds tunnel detection requirements. In order to improve processing efficiency, point cloud should be segmented with start and end mileage as boundaries.

As shown in figure 1, calculate the center point O and normal vector  $V_1$  of tunnel cross-section at a certain mileage based on design information. Wherein, vector  $V_1$  is perpendicular to tunnel cross-section, and this vector points towards the direction of large mileage. For any point P in space, a vector  $V_2$  is formed from point O to point P. A dot product operation is performed on vectors  $V_1$  and  $V_2$ , as shown in formula 1.

$$V_3 = V_1 \cdot V_2 \quad (1)$$

If the magnitude of vector  $V_3$  is positive, it means that point P is located at the large mileage side of point O, otherwise it is located at the small mileage side of point O.

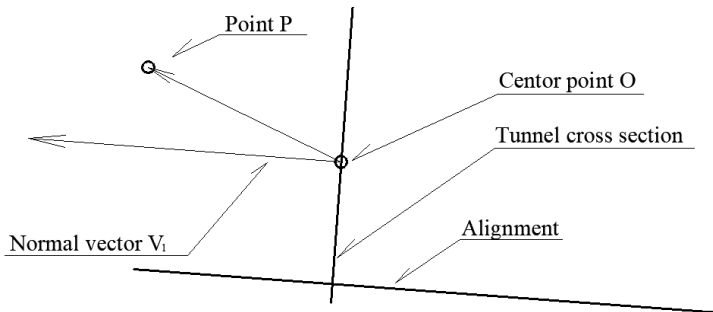


Figure 1. Schematic Diagram of Point Cloud Cutting Elements

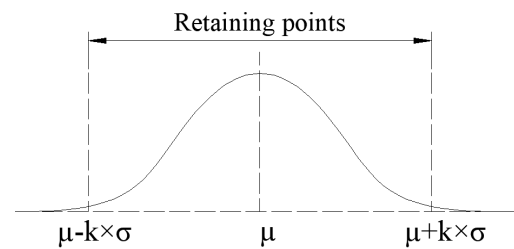


Figure 2. Gaussian Distribution of Point Cloud Spacing

According to above principles, a subset located between the start and end mileage is selected from registered point cloud, and the point cloud segmentation process is finally completed.

### 2.3 Statistical filtering for point cloud denoising

Statistical denoising method<sup>[9]</sup> is adopted in this paper. Supposing the distance between each point and its neighbors inside point cloud follows a Gaussian distribution with mean  $m$  and standard deviation  $s$ , as shown in figure 2.

Let  $i$  and  $j$  be the indices of any point and its any neighboring point in point cloud  $C$ , then the Euclidean distance  $S$  between  $C_i$  and  $C_j$  can be expressed as formula 2.

where  $(X_i, Y_i, Z_i)$  and  $(X_j, Y_j, Z_j)$  are the three-dimensional coordinate values for points  $C_i$  and  $C_j$  respectively. The average Euclidean distance between each point and all points in its neighborhood is denoted by  $\mu_s$ , which can be calculated as formula 3, where  $n$  is the number of points included in neighborhood. The standard deviation is expressed as formula 4.

To control filtering range, a parameter  $k$  is set as the standard deviation multiple. For neighborhood of any point, if Euclidean distance between the point and its neighbor lies within  $(\mu_s - k \cdot \sigma, \mu_s + k \cdot \sigma)$ , it is retained, otherwise it is removed<sup>[10]</sup>.

$$S = \sqrt{(X_i - X_j)^2 + (Y_i - Y_j)^2 + (Z_i - Z_j)^2} \tag{2}$$

$$\mu_s = \frac{1}{n} \sum_{t=1}^n S \tag{3}$$

$$\sigma = \sqrt{\frac{1}{n} \sum_{t=1}^n (S - \mu_s)^2} \tag{4}$$

### 2.4 Voxel grid downsampling

Point cloud downsampling is a process of simplifying the point cloud or reducing its density, ultimately achieving a sparse effect. There are many point cloud downsampling methods, including voxel grid method, systematic sampling, random sampling, farthest point sampling, etc.<sup>[6]</sup>. Various downsampling methods are suitable for different scenarios.

Due to its high computational efficiency and uniform distribution of sampled points, voxel grid method is used for downsampling 3D laser scanning point cloud data in this paper. Firstly, an axis-aligned bounding box (AABB) is established, and then the bounding box is divided into  $n$  equal parts along each coordinate axis. Next, only points with minimum distance to the centroid is retained within each voxel, as shown in figure 3, thus maximizing point cloud authenticity.

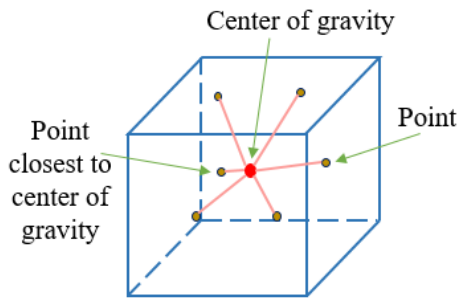


Figure 3. Schematic Diagram of Voxel Downsampling

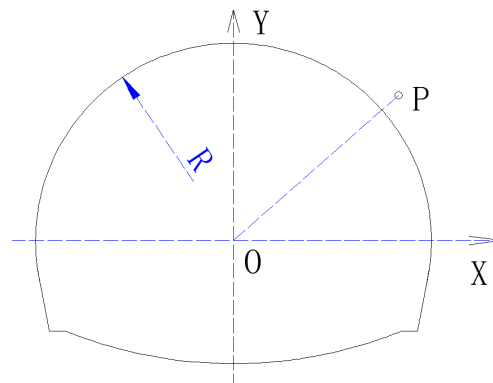


Figure 4. Local Coordinate System of Tunnel Cross Section

## 3. OVER-UNDER EXCAVATION CALCULATION

### 3.1 Calculation of over-under excavation values at each point

As shown in figure 4, a local coordinate system is established at any mileage. In this coordinate system, origin  $O$  coincides with the center of arch crown, whose radius is  $R$ . As the tunnel excavation length is far smaller than spatial radius of the railway's vertical and horizontal curve, in order to improve the over-under excavation calculation efficiency, local coordinate system at the middle of the excavation segment can be used to represent local coordinate system of the whole segment.

Based on design information, calculate vector  $V_1$  representing the local coordinate system origin in the current mileage. And then, rotation matrix  $M_1$  for transformation between the global and local coordinate system is also calculated. Global coordinate value for any point P is represented by vector  $V_2$ , and the formula 5 is used to obtain vector representing its local coordinate value:

In order to project point P onto XOY plane of the local coordinate system, set z-component value of vector  $V'_2$  to 0. Calculate the distance between local coordinate system origin O and point P, and compare this distance with the arch crown radius to obtain over-under excavation value corresponding to point P.

$$V'_2 = (V_2 - V_1) \cdot M_1 \quad (5)$$

### 3.2 DBSCAN point cloud clustering

After calculation of over-under excavation values at each point, it is easy to identify which points are over-excavated and which points are under-excavated. In actual tunnel excavation process, the over- and under-excavation regions are distributed intermittently. To calculate the volume of each region, DBSCAN algorithm is used to cluster the over-excavation and under-excavation points separately, acquiring several continuous regions.

Point cloud clustering is an unsupervised problem that can discover the intrinsic structural information hidden in data set and divide regions with high similarity into one class. Clustering methods are usually classified into tree clustering, partitioning clustering, density-based, grid-based clustering algorithms, and other clustering algorithms. DBSCAN is a classical representative of density-based algorithms, which can discover point clusters of arbitrary shapes and is less affected by noise and outliers.

MinPts (clustering density) and  $\epsilon$ (clustering radius) are two important parameters of DBSCAN algorithm. For a given point set  $D=\{X_1, X_2, \dots, X_m\}$ , under the condition of MinPts=3, basic concepts of DBSCAN clustering algorithm can be described through spatial distribution characteristics of four points  $X_1, X_2, X_3$ , and  $X_4$ , as shown in figure 8. The circular dotted line with radius  $\epsilon$  in the figure represents  $\epsilon$ -neighborhood. Except for  $X_1$  itself, there are three points in the  $\epsilon$ -neighborhood of  $X_1$ , which is not less than MinPts and belongs to core object. Point  $X_2$  is directly density-reachable from object  $X_1$  since it is located within the  $\epsilon$ -neighborhood range of point  $X_1$ . Point  $X_3$  is directly density-reachable from  $X_2$  and indirectly density-reachable from object  $X_1$ .  $X_3$  is connected by density to  $X_4$ .

Taking over-excavation as an example, the idea of using DBSCAN algorithm to obtain continuous over-under excavation regions is introduced as follows: first, randomly choose a point from the over-excavation dataset as a seed, and then find all the core objects based on given clustering density MinPts value and clustering radius  $\epsilon$ . Then, starting from any core object, find the density-reachable sample set from it to generate a cluster, and continue until all core objects are accessed. The result of each cluster represents a continuous over-excavation region.

### 3.3 Ball Pivoting point cloud triangulation

Surface reconstruction methods based on scattered point clouds can be mainly divided into three categories: Delaunay triangulation based methods, implicit surface reconstruction, and region-growing methods. Among them, region-growing methods first start with a seed triangle as initial mesh, and extends the initial mesh by obtaining a third point based on a certain topological criterion, until all points are traversed, finally the reconstructed surface is generated. This method possesses advantages of low time complexity, and cable of handling large-scale point clouds. Commonly used region-growing algorithms include ball pivoting algorithm (BPA), intrinsic property driven algorithm (IPD), bounding sphere algorithm, and poisson meshing algorithm.

Since the input point cloud spatial position does not change during surface reconstruction process, the accuracy of over- and under-excavation volume calculated can be guaranteed. In this paper, Ball Pivoting algorithm (BPA)<sup>[11]</sup> is used for point cloud triangulation. The principle of this algorithm is as follows:

Firstly, define a sphere with radius r. When the sphere rolls and touches a point, and the sphere does not contain any other points, a triangle is formed by connecting the point to rotational axis. BPA starts with a seed triangle, and the sphere rolls along one of its edges (rolling along the edge while maintaining contact with endpoints of the edge) until the sphere touches the next point, and then a triangle is formed by connecting that edge with the newly touched point.

Assume that M is the surface of an object and S is a set of sampled points on the object. Supposing the points are dense enough so that a sphere with radius r cannot pass through the surface without touching a sample point. Starting with a mesh composed of a seed triangle, the sphere is kept in contact with both points of each edge on the boundary of the seed

triangle, and then rotated until encountering a new point. Then, a new triangle and a new mesh boundary are formed by connecting the edge with the point. This process is repeated until all edges are visited. If there are still unvisited points, a seed triangle is selected from the set of unvisited points, and repeat above process.

### 3.4 Over-under excavation volume calculate based on triangle mesh projection

After point cloud triangulation is completed using BPA algorithm, a TriangleMesh object is generated, which has two important properties: the triangles property stores all triangles that make up the mesh in form of array, and each triangle is represented by its three nodes; the vertices property stores all nodes of the mesh in form of array, and each node is represented by its x, y, and z coordinate values. As above-mentioned, the global coordinates, local coordinates, and over-under excavation values of input point cloud can be calculated through coordinate transformation. As shown in figure 5, using a relational database strategy, association is established between TriangleMesh, triangles, vertices, and the over-under excavation values of each point based on global x, y, and z coordinate values as foreign keys.

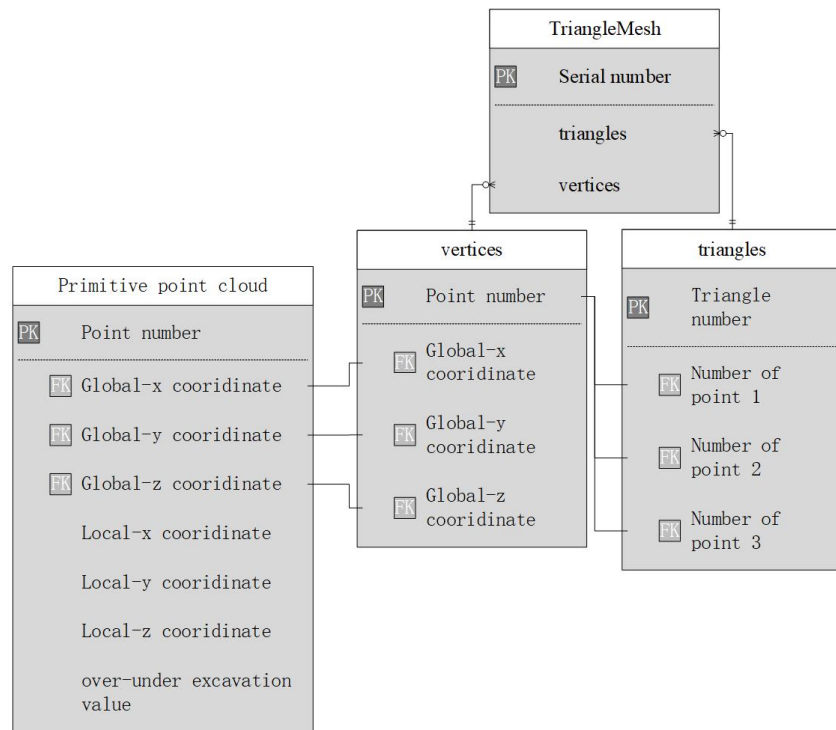


Figure 5. Relationship between Triangulated Mesh and Primitive Point Cloud Data

As shown in figure 6, for any triangle ABC in the mesh, DEF is the one projected onto inner contour of the tunnel. Calculate the area  $s$  of triangle DEF and the distance  $h$  between centroids of the two triangles. The over- and under-excavation volume of each triangle can be expressed as a prism.

For each point cloud cluster, traverse all the triangles in the mesh and perform above operations iteratively to generate volume of each continuous over-under excavation region.

## 4. ENGINEERING APPLICATION

### 4.1 Engineering overview

One underwater railway tunnel in southern China has a designed speed of 350 km/h, a single tunnel with two tracks, whose total length is 9,257 meters. Mining methods are used for construction. This tunnel runs through multiple active fault zones in an eroded hilly area, and the ground has large undulations. Site surface is covered by Quaternary Neogene deposits and rock formations such as Yan Mountain and Xi Mountain.

3D laser scanner is used to detect the over-under excavation conditions in segment from DK155+519.50 to DK155+539.50, whose length is about 20 meters.

## 4.2 Point cloud data preprocessing

Due to the large amount of point cloud data initially collected, which contains a lot of irrelevant information, spatial vector analysis is used with the aid of alignment elements from tunnel plan and longitudinal profile data to cut the point cloud within excavation range, highly improving efficiency and accuracy. A statistical filtering method is used with aforesaid cutting result as input to complete noise removal. To address the missing phenomenon caused by non-relevant point clouds of wind tube after denoising, a deep learning model based on dynamic graph convolutional network is used to complete point cloud. A voxel grid downsampling method is used with voxel edge length of 10 mm. In this method, point closest to the center of gravity within the voxel is to replace current voxel, reducing point cloud density. Results of each step in point cloud preprocessing are shown in figure 7.

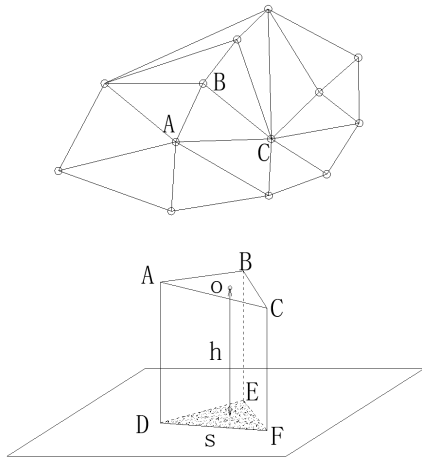


Figure 6. Schematic Diagram of Triangulated Mesh and Projected Prism

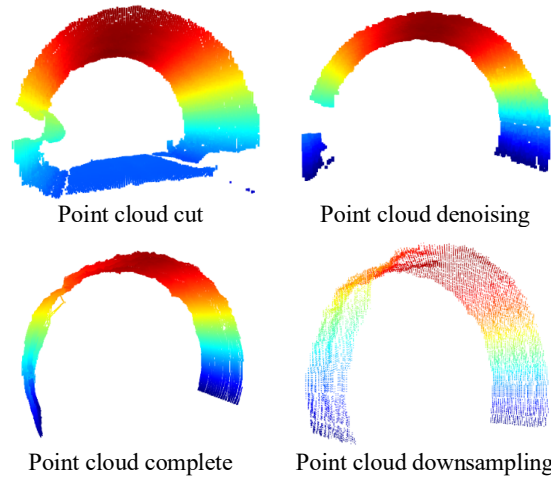


Figure 7. Results of Point Cloud Data Preprocessing

## 4.3 Calculation of over-under excavation volumes

Using the alignment and cross-sectional information of the tunnel, point cloud on tunnel surface is converted from global coordinate system to local coordinate system to calculate the over-under excavation values at each point. DBSCAN algorithm is used to cluster the points of over-excitation and under-excitation separately, and to obtain several continuous over-under excavation regions. BPA algorithm is used to triangulate each point cloud of the clustering. All triangle meshes are traversed and projected onto the tunnel contour, and the over-under excavation volume calculation is completed through prism volume integration. Results of over-under excavation volume calculation are shown with a cloud map and statistical analysis list in figure 9.

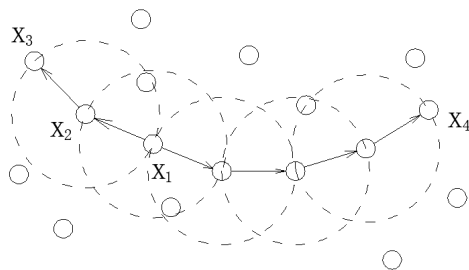


Figure 8. Schematic Diagram for DBSCAN Basic Concepts

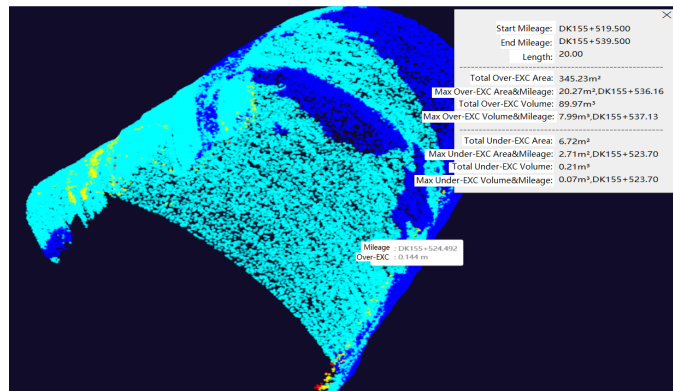


Figure 9. Calculation and Statistics Results of Over-Excavation

## 5. CONCLUSION

3D laser scanning technology does not require the layout of monitoring stations, and can collect tunnel surface data densely, comprehensively, efficiently while meeting accuracy requirements. This technology also improves the automation level of quality inspection and the efficiency during tunnel construction. Based on point cloud obtained from 3D laser scanning, this study conducted research on point cloud data preprocessing and over-under excavation volume calculation technology, finally conducted an application verification. Conclusions are as follows:

- This paper researched point cloud registration technology based on ICP algorithm, point cloud cutting technology based on spatial vector analysis, point cloud statistical filtering noise removal algorithm, and point cloud voxel grid downsampling method, achieving preprocessing of the primitive collected point cloud data.
- By converting global coordinate system to local one and calculating over-under excavation value at each point, DBSCAN algorithm was used to cluster point cloud based on their over-under excavation attributes. BPA algorithm was used to triangulate the point cloud of each cluster, and over-under excavation volume calculation was achieved based on triangle mesh projection technology.
- Research results were applied in one underwater railway tunnel construction in southern China to achieve over-under excavation calculation for a 20-meter length tunnel segment constructed using mining methods.

## ACKNOWLEDGMENT

The authors gratefully appreciate support from the Science and Technology Development Project of China National Railway Group Co., Ltd(No. N2022G064), and the Science and Technology Development Project of Jing Jin Ji Intercity Rapid Railway Investment Co., Ltd (No. JJJ2022A01).

## REFERENCES

- [1] L.E. Carter-Greaves, M. Eyre, D. Vogt, etc. Algorithm development for automated key block analysis in tunnels from LiDAR point cloud data[J]. *Tunnelling and Underground Space Technology*, 2023, 132, 104787. <https://doi.org/10.1016/j.tust.2022.104787>.
- [2] Tsukasa Mizutani, Takahiro Yamaguchi, Tomoshi Kudo, etc. Quantitative evaluation of peeling and delamination on infrastructure surfaces by laser signal and image processing of 3D point cloud data[J]. *Automation in Construction*, 2022, 133, 104023. <https://doi.org/10.1016/j.autcon.2021.104023>.
- [3] Y. Li, Y. Zhuo, Y.S. Wu, etc. Application of Over-Under-Cut Algorithm in Tunnel Excavation Based on 3D Laser Scanning Technology[J]. *RAILWAY STANDARD DESIGN*, 2021, 65(10):200-204. DOI:10.13238/j.issn.1004-2954.202106300006.
- [4] L. Xu, C.J. Wang. Research on the Detection Method of Tunnel Under-over Break Using Point Cloud[J]. *JOURNAL OF RAILWAY ENGINEERING SOCIETY*, 2016, 33(12) : 77-81. [https://kns.cnki.net/kcms2/article/abstract?v=FbDnLXx9-bly219SBR6NMZZ34jii9M8EKvPYxP5d2fRR-FEPmzEHmZoESdEyBZD39h2q-de0jYuTed\\_qYamMwDIjb7X1BIHJcERcY98eaRn7C7Uus4yBSEuUsOQa1tshnr\\_6CIlnK98=&uniplatform=NZKPT&language=CHS](https://kns.cnki.net/kcms2/article/abstract?v=FbDnLXx9-bly219SBR6NMZZ34jii9M8EKvPYxP5d2fRR-FEPmzEHmZoESdEyBZD39h2q-de0jYuTed_qYamMwDIjb7X1BIHJcERcY98eaRn7C7Uus4yBSEuUsOQa1tshnr_6CIlnK98=&uniplatform=NZKPT&language=CHS).
- [5] X.L. Zheng. A Laser Scanning Method for the Detection of Tunnel Over-Under Excavation. *Urban Geotechnical Investion&Surveying*, 2022(1):145-148. [https://kns.cnki.net/kcms2/article/abstract?v=FbDnLXx9-bkWct9BhzbIpPXTaZNXGW3g\\_JYATer1s2FyaGUpMjI\\_x4Jx3aUxOCd-hA5vwFKG8Z8-GaXsFvc7QTscSeOT9U5YfKB6hflFrgeSyTDZA-CRf8ZFPzFg\\_kqZEX9-opxbqA=&uniplatform=NZKPT&language=CHS](https://kns.cnki.net/kcms2/article/abstract?v=FbDnLXx9-bkWct9BhzbIpPXTaZNXGW3g_JYATer1s2FyaGUpMjI_x4Jx3aUxOCd-hA5vwFKG8Z8-GaXsFvc7QTscSeOT9U5YfKB6hflFrgeSyTDZA-CRf8ZFPzFg_kqZEX9-opxbqA=&uniplatform=NZKPT&language=CHS).
- [6] L.E. Carter-Greaves, M. Eyre, D. Vogt, etc. Algorithm development for automated key block analysis in tunnels from LiDAR point cloud data[J], *Tunnelling and Underground Space Technology*, 2023, 132, 104787, <https://doi.org/10.1016/j.tust.2022.104787>.
- [7] F.A. Donoso, K.J. Austin, P.R. McAree. How do ICP variants perform when used for scan matching terrain point clouds?[J], *Robotics and Autonomous Systems*, 2017, 87: 147-161, <https://doi.org/10.1016/j.robot.2016.10.011>.

- [8] Daniel Lopez, Carl Haas, Sriram Narasimhan. Specific object finding in point clouds based on semantic segmentation and iterative closest point[J]. Automation in Construction. 2013, 156, 105116, <https://doi.org/10.1016/j.autcon.2023.105116>.
- [9] B. Liu, X.M. Li. A Self-Adaptive Dual Radius Filtering Algorithm Based on LIDAR Point Cloud[J/OL]. Acta Armamentarii 1-9. <http://kns.cnki.net/kcms/detail/11.2176.TJ.20230515.1134.002.html>.
- [10] R.Z. Li, M. Yang, Y. Ran, etc. Point Cloud Denoising and Simplification Algorithm Based on Method Library[J]. Laser & Optoelectronics Progress. 2018, 55(1): 243-249. [https://kns.cnki.net/kcms2/article/abstract?v=FbDnLXx9-blbNaO2vc3aPLYFIHuL8RU5oWq4F059bPLIZ9ZE-8mObeJijIpngTH9yZC4jYyHp1\\_o5GZ72831Hv1BJYypw0BwnMb2lrpGDzPsoOmjFUdbV98gSYZ2LMiy4P1k2rm\\_ICI=&uniplatform=NZKPT&language=CHS](https://kns.cnki.net/kcms2/article/abstract?v=FbDnLXx9-blbNaO2vc3aPLYFIHuL8RU5oWq4F059bPLIZ9ZE-8mObeJijIpngTH9yZC4jYyHp1_o5GZ72831Hv1BJYypw0BwnMb2lrpGDzPsoOmjFUdbV98gSYZ2LMiy4P1k2rm_ICI=&uniplatform=NZKPT&language=CHS).
- [11] J. Digne, An Analysis and Implementation of a Parallel Ball Pivoting Algorithm, Image Processing On Line, 4 (2014): 149–168. <https://doi.org/10.5201/ipol.2014.81>.